

# Modelling of fast jet formation under explosion collision of two-layer alumina/copper tubes

**I Balagansky<sup>1\*</sup>, A Vinogradov<sup>1</sup>, L Merzhievsky<sup>2</sup>**

1. Novosibirsk State Technical University, Russia,

2. Institute of Hydrodynamics SB RAS, Russia

## ABSTRACT

Under explosion collapse of two-layer tubes with an outer layer of high-modulus ceramics and an inner layer of copper, formation of a fast and dense copper jet is plausible. We have performed a numerical simulation of the explosion collapse of a two-layer alumina/copper tube using ANSYS AUTODYN software. The simulation was performed in a 2D-axis symmetry posting on an Eulerian mesh of 3900x1200 cells. The simulation results indicate two separate stages of the tube collapse process: the nonstationary and the stationary stage. At the initial stage, a non-stationary fragmented jet is moving with the velocity of leading elements up to 30 km/s. The collapse velocity of the tube to the symmetry axis is about 2 km/s, and the pressure in the contact zone exceeds 700 GPa. During the stationary stage, a dense jet is forming with the velocity of 20 km/s. Temperature of the dense jet is about 2000 K, jet failure occurs when the value of effective plastic deformation reaches 30.

## 1. INTRODUCTION

It is known [1-3] that formation of condensed jets capable of penetrating targets is possible only if the collision point moves with velocity  $V_c$  not greater than bulk speed of sound in the liner material  $C_b$

$$V_c \leq C_b. \quad (1)$$

At the same conditions, formation of dense cumulative jets from cylindrical liners (tubes) is possible [4]. Since the collision point velocity  $V_c$  for the cylindrical liner is equal to the detonation velocity of the HE charge  $U_D$

$$V_c = U_D, \quad (2)$$

the necessary condition for obtaining a condensed cumulative jet from a cylindrical liner is

$$C_b \geq U_D. \quad (3)$$

The maximum velocity attainable by a shaped charge jet was estimated by S.A. Kinelovskii and Yu.A. Trishin (1980) [2], Carleone and Chou (1981) [3]

$$V_j \leq 2.41C_b. \quad (4)$$

\*Corresponding Author: balaganskij@corp.nstu.ru

Thus, materials having speed of sound greater than detonation velocity in HE charges prove to be interesting for research. Obviously, the most interesting are ceramic materials that have such unique properties as high values of wave process velocities and Hugoniot elastic limit, indicating the possibility of transmission of significant disturbances by elastic waves.

Usage of acceleration devices based on HE charges containing alumina ceramic tubes for generation of ceramic streams with velocities up to 11.0 - 12.4 km/s was experimentally substantiated in paper [5]. Theoretical velocity limit was estimated as 19.0 km/s for alumina and 32.5 km/s for BN.

Figure 1 shows the movement of a cumulative jet formed from an alumina ceramic tube [5]. One can see that the jet is a flow of dispersed ceramic particles. The particles have a substantial radial velocity, which leads to reduction of flow density.

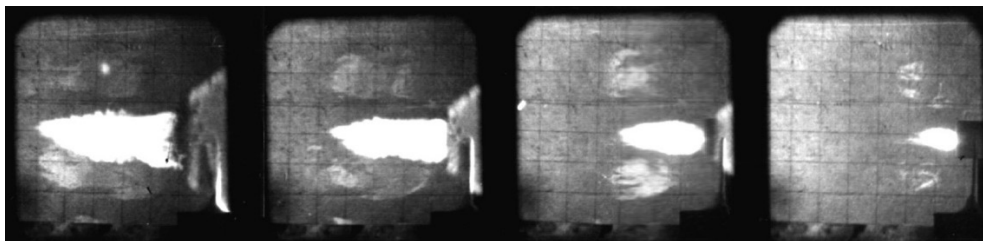


Figure 1. Cumulative jet movement in air. Grid cell size is 25x25 mm. Time difference between pictures is 2.66  $\mu$ s

## 2. COMPUTER SIMULATION

In our opinion, explosion collapse of two-layer tubes with an outer layer of high-modulus ceramics and an inner layer of copper can produce a fast and dense copper jet. We have performed a numerical simulation of an explosion collapse in a two-layer alumina/copper tube. The simulation using ANSYS AUTODYN software was performed in a 2D-axis symmetry posting on an Eulerian mesh of 3900x1200 cells. The spatial resolution was 30 cells per mm. A detonation wave was initiated as a plane wave and propagated from the left to the right boundary of the mesh. Boundary conditions on the left, right, and upper boundaries were defined in terms of AUTODYN as "Flow out." We used values of material parameters from the AUTODYN EOS library.

Table 1: Main parameters of the equations of state for materials

Material Name	Equation of State	Strength	Failure
AL 921-T	Shock	None	None
COMP B 163	JWL	None	None
Copper1	Shock	Johnson Cook	None
AL2O3 CERA	Shock	von Mises	None
STEEL 1006	Shock	Johnson Cook	None

Initial posting with dimensions of 130x40 mm is shown in Figure 2. Detonation was initiated on the left face of the HE charge. The simulation results are given in the form of contour lines, flow fields, space and time profiles.

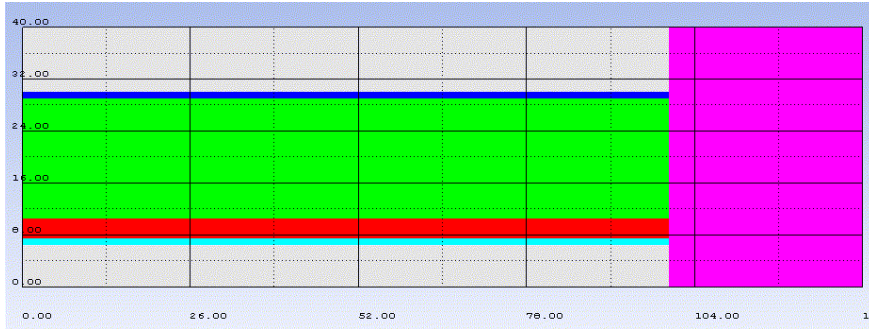


Figure 2. Initial posting with dimensions of 130x40 mm. Aluminum shell is shown in dark blue; HE charge - green; ceramic tube - red; copper tube - light blue; steel target - purple.

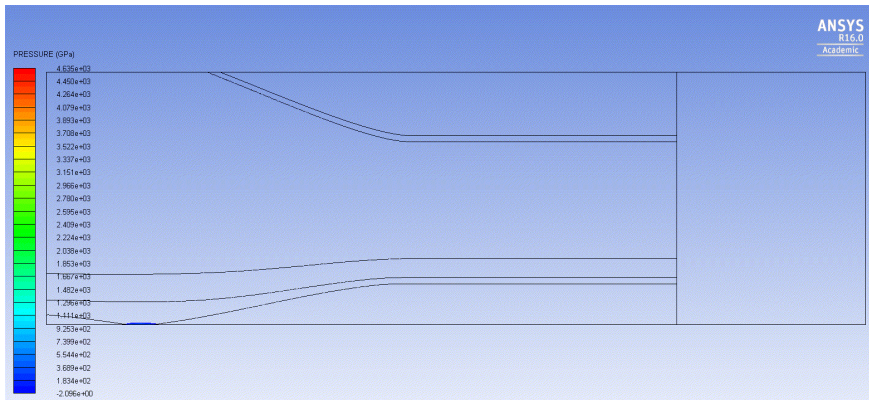


Figure 3. Material flow fields and pressure contours at the time of the collapse of the tube to symmetry axis at  $t=7.6 \mu s$

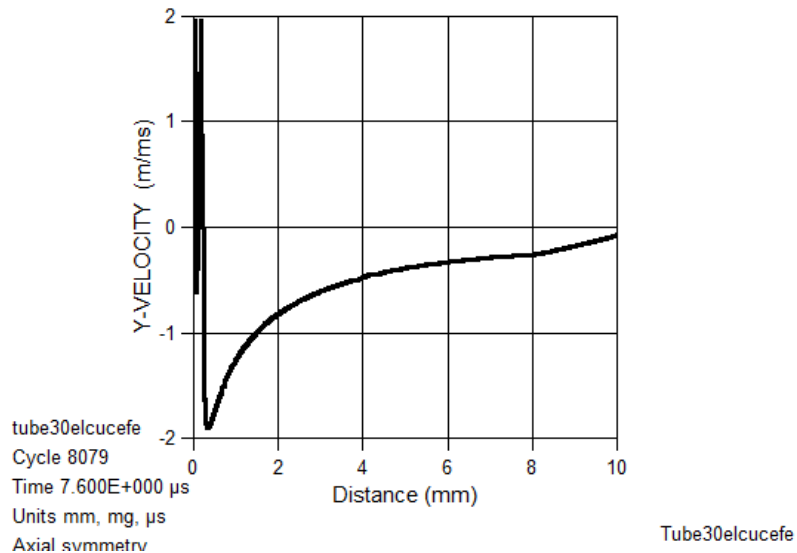


Figure 4. Radial velocity profiles vs. tube thickness from 0 to 10 mm,  $t=7.6 \mu s$

Figure 3 shows the flow field and pressure contours at the time of the collapse of the tube to the symmetry axis at  $t=7.6 \mu\text{s}$ . Figure 4 shows the distribution of the radial velocity versus the liner thickness from 0 to 10 mm at  $t = 7.6 \mu\text{s}$ . On Figure 5, the pressure distribution is given versus the lining thickness from 0 to 10 mm at  $t = 7.6 \mu\text{s}$ . One can see that the tube collapses to its symmetry axis with a velocity of about 2 km/s, and pressure value exceeds 700 GPa at this time.

Material flow fields and pressure contours at  $t=8.5 \mu\text{s}$  are given on Figure 6.

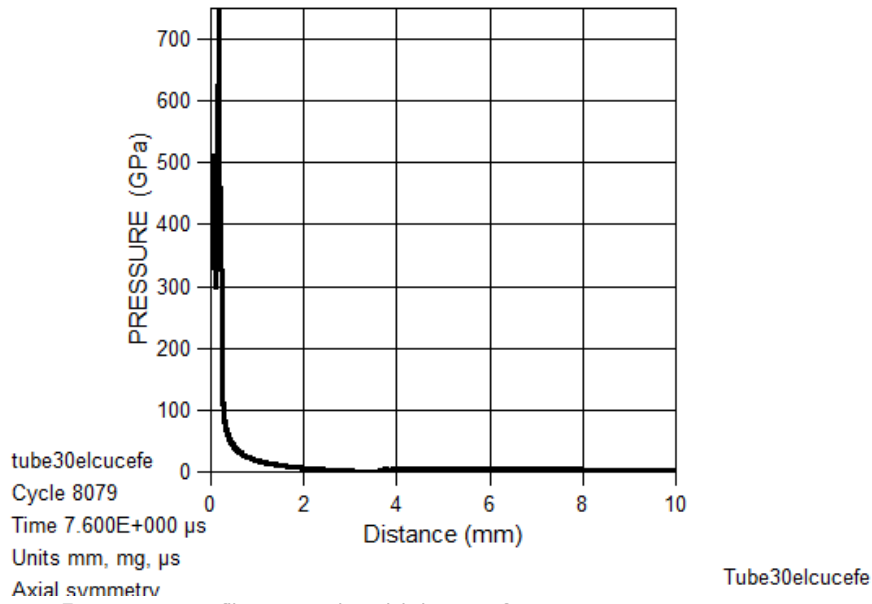


Figure 5. Pressure profiles vs. tube thickness from 0 to 10 mm,  $t=7.6 \mu\text{s}$

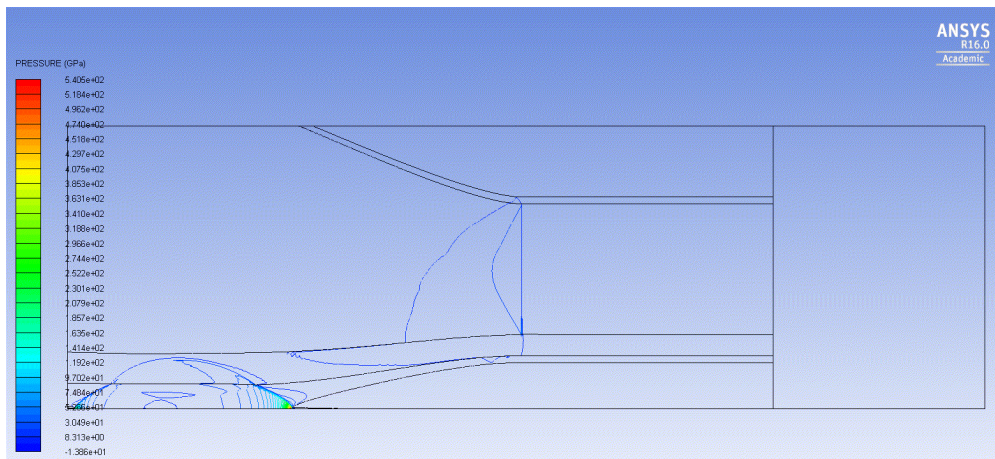


Figure 6. Material flow fields and pressure contours at  $t=8.5 \mu\text{s}$ .

Mass velocity and pressure profiles along the symmetry axis from 25 to 50 mm are given on Figures 7 and 8, respectively.

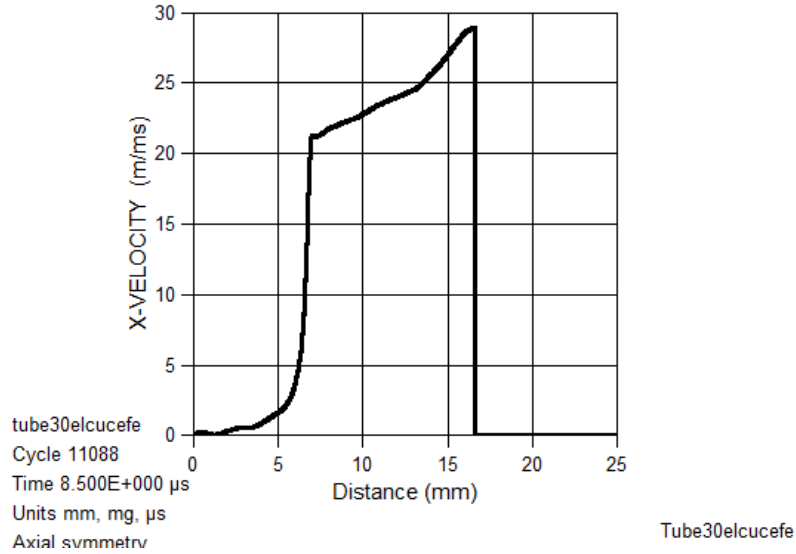


Figure 7. Mass velocity profile along the symmetry axis from 25 to 50 mm at t=8.5 μs

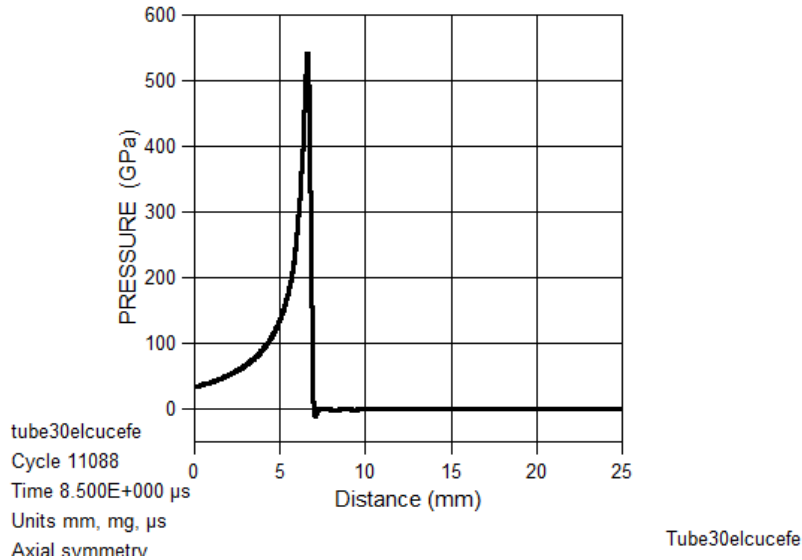


Figure 8. Pressure profile along the symmetry axis from 25 to 50 mm at t=8.5 μs

The velocity value along the length of the jet varies from 21.3 to 28.9 mm/μs. Maximum pressure reaches 540 GPa. The process of the collapse of the tube has a non-stationary behavior.

Figure 9 shows the flow fields and pressure contours at the beginning of the process of the jet penetration into the target at time t=10.7 μs. Figures 10 and 11 show the velocity and

pressure distribution respectively versus the jet length. Figures 12 and 13 show the temperature distribution and the effective plastic strain along the length of the jet at the same time.

One can see that the leading part of the jet, formed at non-stationary stage, is discontinuous and consists of individual fragments. The leading portion of the dense stream moves at velocity of about 20 mm/ $\mu$ s. The temperature of the dense stream is about 2000 K, jet failure occurs when the value of the effective plastic strain is about 30.

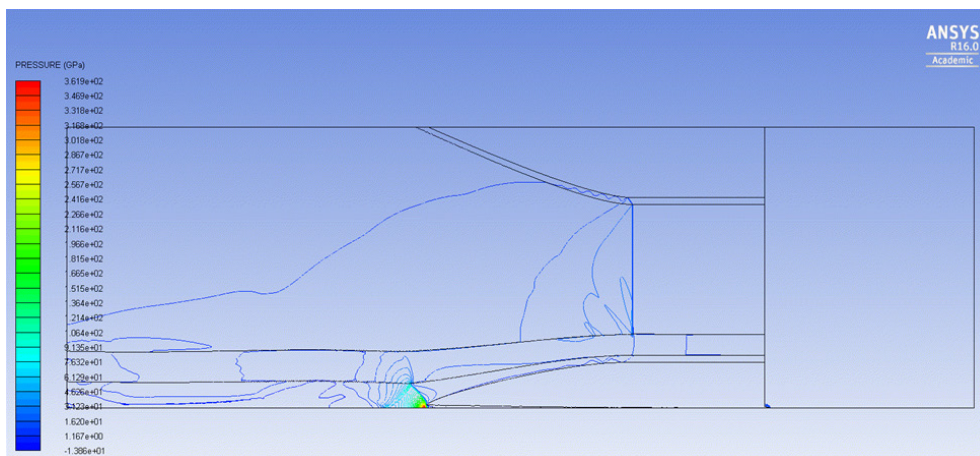


Figure 9. Material flow fields and pressure contours at the beginning of process of jet penetration into target  $t=10.7\mu$ s

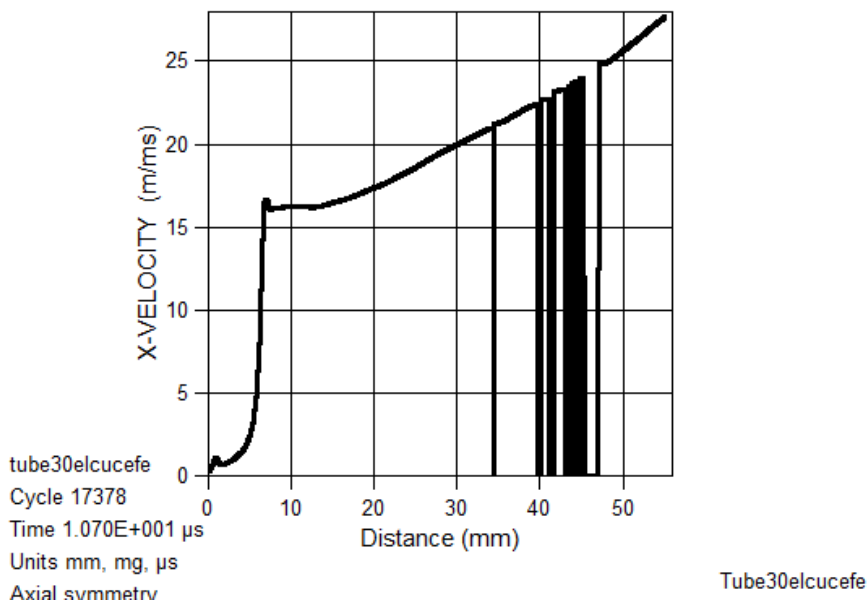


Figure 10. X-velocity distribution vs. the jet length from 50 to 100 mm,  $t=10.7\mu$ s

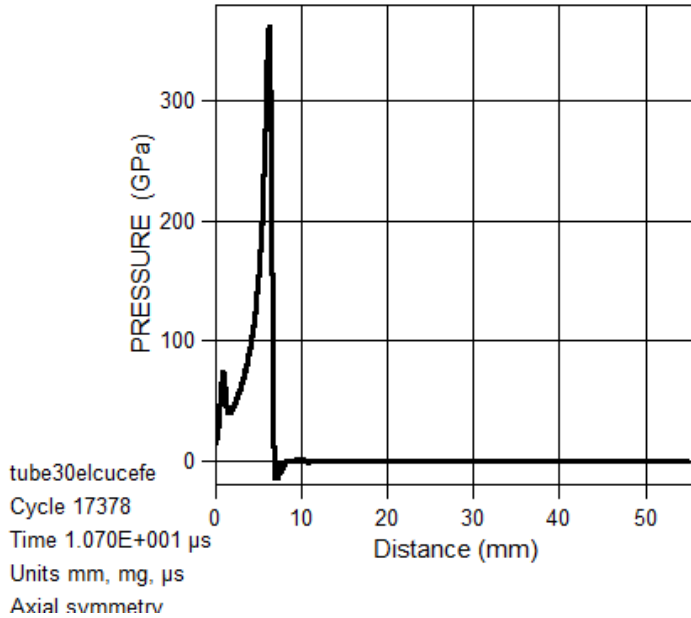


Figure 11. Pressure distribution respectively vs. the jet length from 50 to 100 mm,  $t=10.7\mu$ s

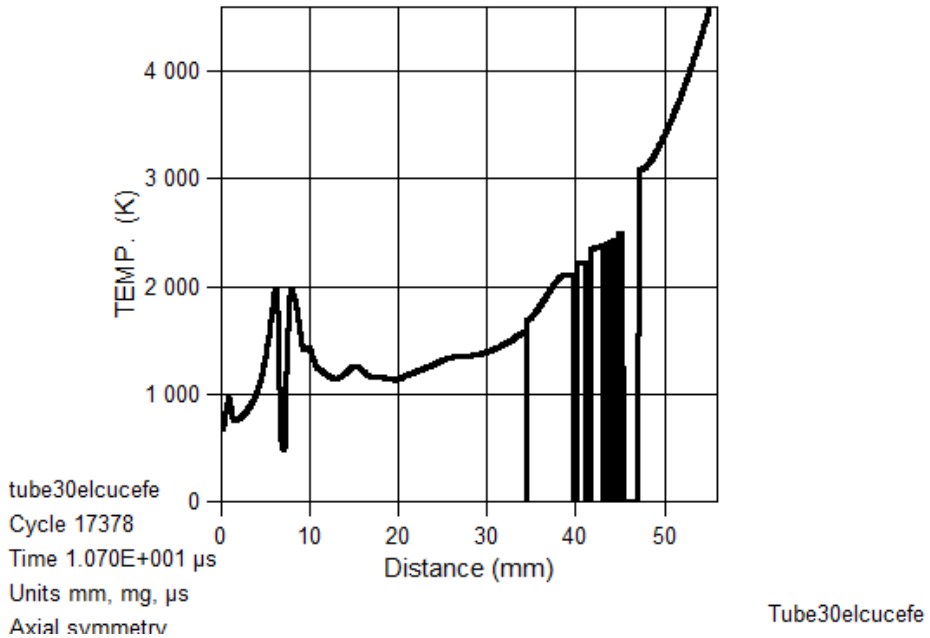


Figure 12. Temperature distribution along the length of the jet from 50 to 100 mm,  $t=10.7\mu$ s

Figure 14 shows the flow fields and pressure contours at the end of the jet penetration into the target at time  $t=14.5 \mu$ s.

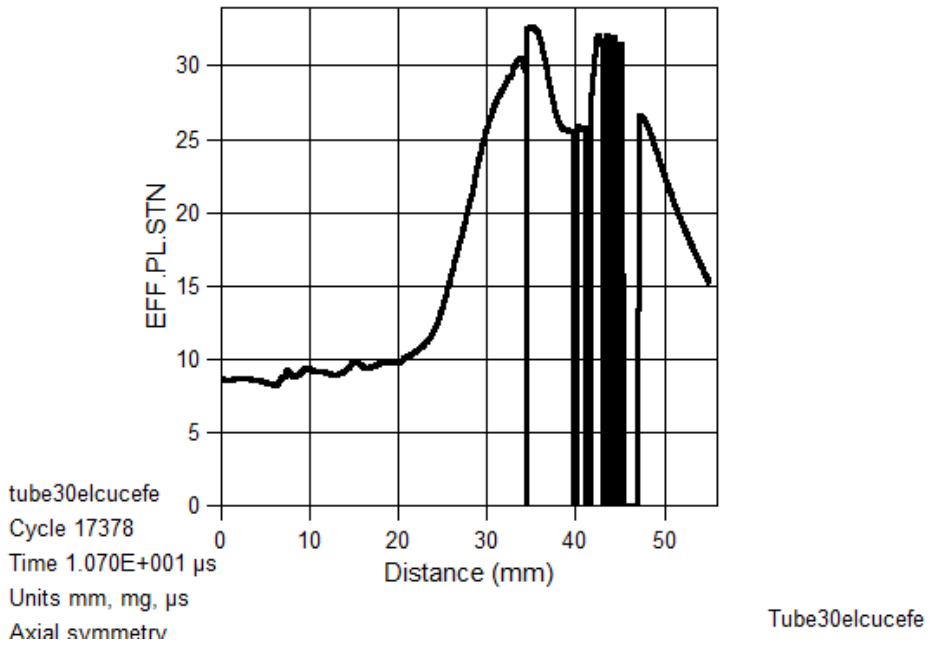


Figure 13. Effective plastic strain distribution along the length of the jet from 50 to 100 mm,  $t=10.7\mu s$

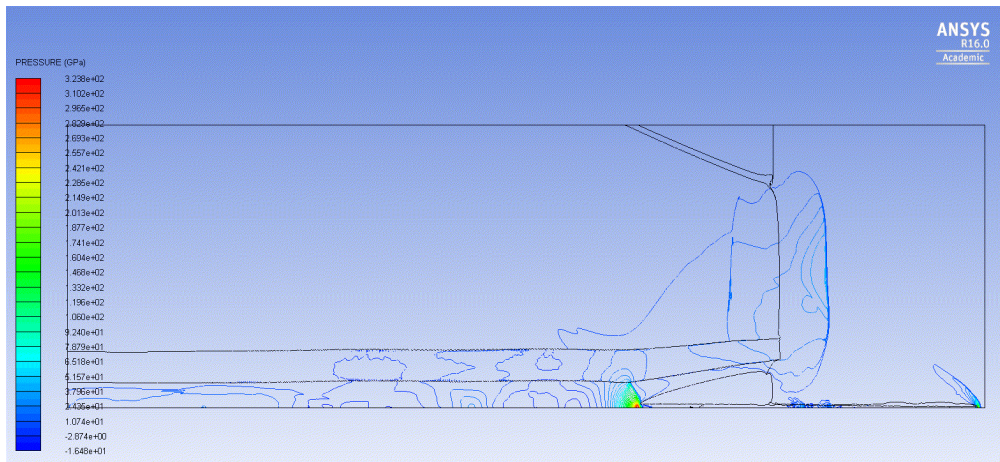


Figure 14. Flow fields and pressure contours at time  $t=14.5\mu s$

Figures 15 - 18 show the x-velocity, pressure, temperature and effective plastic strain distribution along the length of the jet from 75 to 130 mm at the same time.



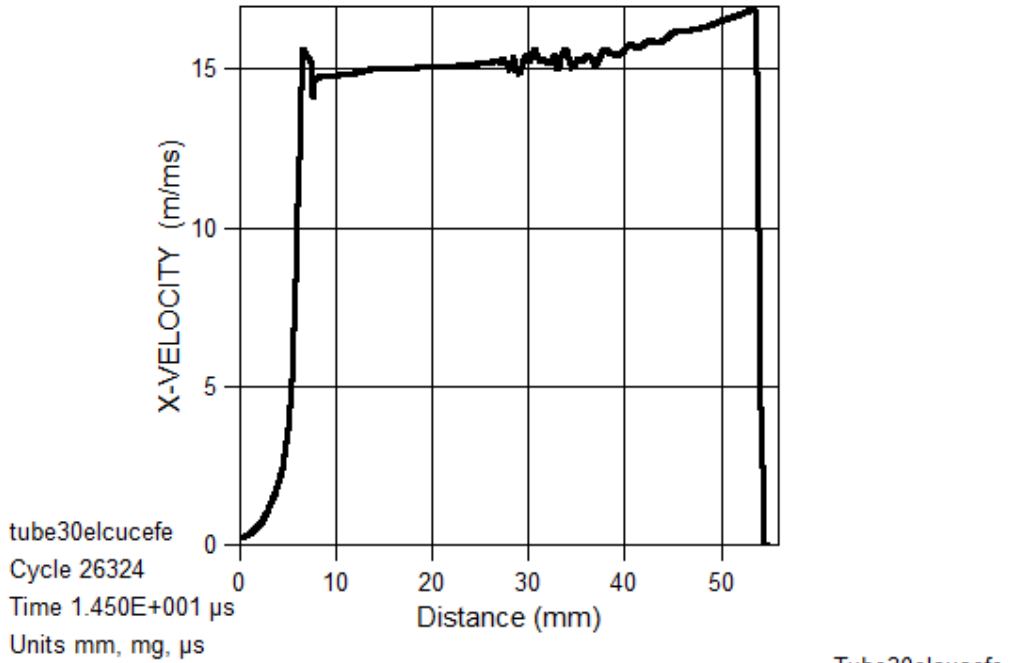


Figure 15. X-velocity distribution along the length of the jet from 75 to 130 mm,  $t=14.5 \mu$ s

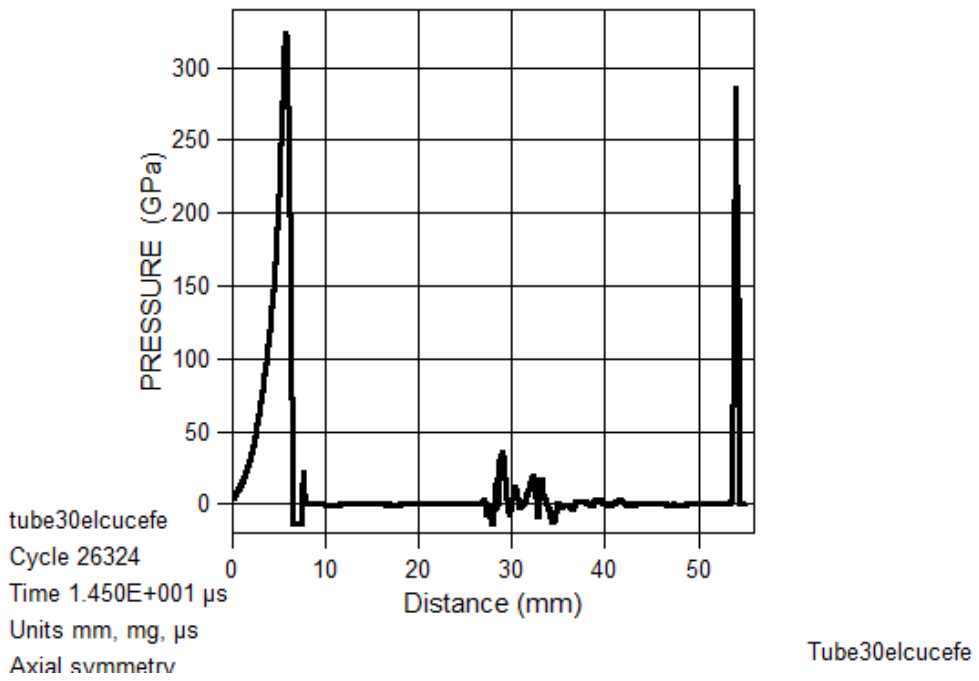


Figure 16. Pressure distribution along the length of the jet from 75 to 130 mm,  $t=14.5 \mu$ s

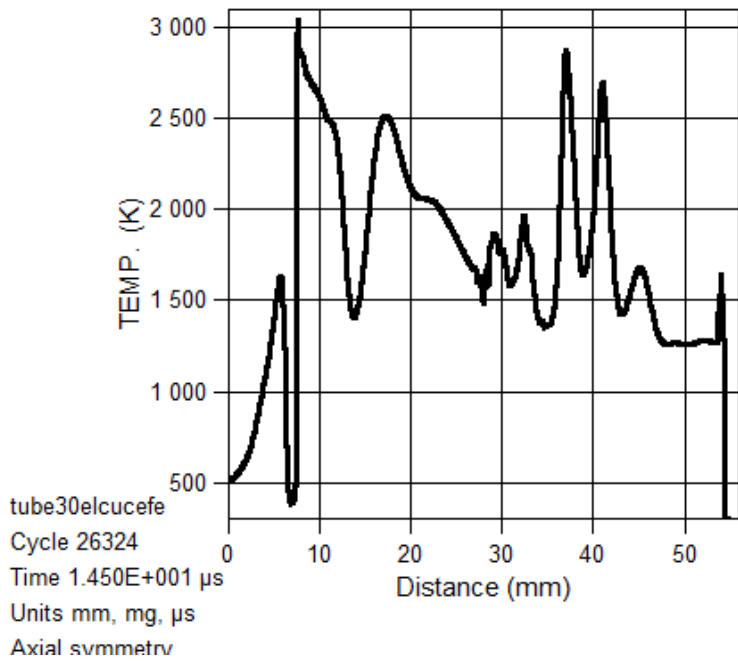


Figure 17. Temperature distribution along the length of the jet from 75 to 130 mm,  $t=14.5 \mu$ s

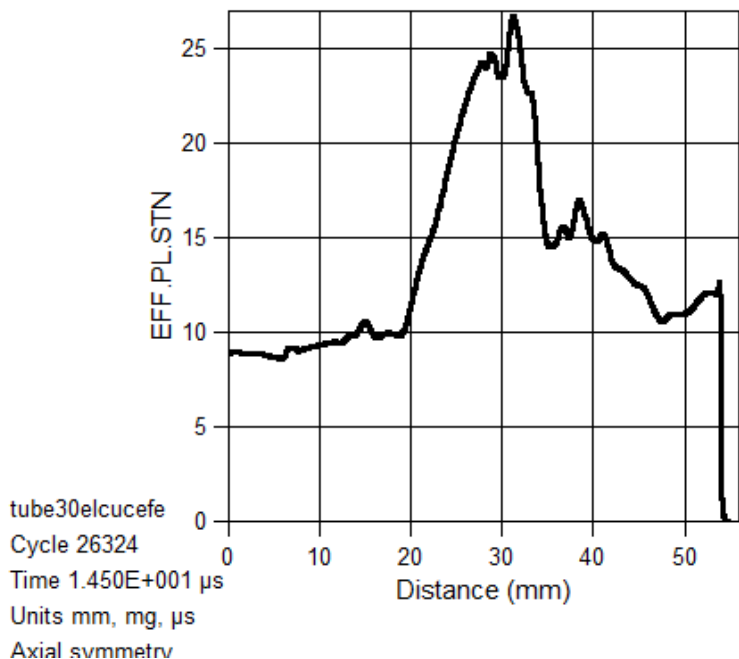


Figure 18. Effective plastic strain distribution along the length of the jet from 75 to 130 mm,  $t=14.5 \mu$ s

#### **4. CONCLUSIONS**

The simulation results indicate two separate stages of the process: the nonstationary and the stationary stage. Initially, a non-stationary fragmented jet moves with the velocity of leading elements up to 30 km/s. The collapse velocity of the tube to the symmetry axis is about 2 km/s, and pressure in the contact zone exceeds 700 GPa. During the stationary stage, a dense jet forms with the velocity of 20 km/s. Temperature of the dense jet is about 2000 K, jet failure occurs when the value of effective plastic deformation reaches 30.

#### **ACKNOWLEDGEMENT**

This work is supported by the Russian Foundation for Basic Research (Project No. 14-08-00068).

#### **REFERENCES**

- [1] R. Shell, Detonation Physics, in High-Speed Physics, pt.2, 276-349 (1967)
- [2] S.A. Kinelovskii, Yu.A. Trishin: Combustion, Explosion, and Shock Waves, Vol. 16 (1980), pp 504-515
- [3] W.P. Walters, J.A. Zukas, Fundamentals of shaped charges. Willey-Interscience Publication (1989)
- [4] Yu.A. Trishin: J. of Appl. Mech. and Tech. Phys. Vol. 41 (2000), pp 773-787
- [5] I.A. Balagansky, V.A. Agureikin, I.F. Kobilkin et al.: Int. J. of Impact Eng., Vol. 22 (1999), pp 813-823

